Applied Mathematical Modelling 109 (2022) 341–357

Contents lists available at ScienceDirect

Applied Mathematical Modelling

journal homepage: www.elsevier.com/locate/apm

Path tracking control of a tractor-trailer wheeled robot kinematics with a passive steering angle

Yusheng Zhou [a], Kwok-wai Chung [b,*]

[a] School of Mathematics and Statistics, Guizhou University, Guiyang 550025, China
[b] Department of Mathematics, City University of Hong Kong, 83 Tat Chee Avenue, Kowloon Tong, Hong Kong, China

ARTICLE INFO

Article history:
Received 3 August 2021
Revised 18 April 2022
Accepted 25 April 2022
Available online 5 May 2022

Keywords:
Tractor-trailer wheeled robot travelling at a low speed
Non-holonomic constraint
Motion law
Passive steering angle
Relative curvature
Dynamic tracking target

ABSTRACT

In the present work, we propose a trajectory tracking control method for the tractor-trailer wheeled robot in that both the trailer and the tractor are able to precisely track an identical target trajectory curve at a low speed. To this end, two key innovations are presented as follows. Firstly, a passive steering angle and its gear steering mechanism are introduced for steering the trailer, so that it follows very well the trajectory of the tractor. Secondly, the motion laws of the tractor-trailer wheeled robot with a passive steering angle are established by analyzing the non-holonomic constraints. On this basis, a standard method is applied to establish its kinematics and dynamics models. The original motion task of the tractor-trailer wheeled robot is then transformed into a curvature tracking control issue of the tractor via a dynamic tracking target. Finally, the integral sliding mode control and the linear quadratic regulator are combined to design two proper torque controllers for implementing a prescribed motion task. Numerical simulation results show that both the tractor and the trailer can accurately move along the desired path simultaneously by adopting a dynamic tracking target and an appropriate passive steering angle, even though the tracking speed error of the tractor is large.

1. Introduction

Owing to its low energy consumption and high payload capacity, a tractor-trailer wheeled vehicle plays an increasing role in various applications such as public transportation, delivery systems and crop harvesting [1,2]. In theory, multiple trailers can bring significant economic benefits. However, they are easy to cause traffic accidents due to bad lateral stability at high speeds and poor controlled movement at low speeds, especially when taking a sharp turn [3,4]. In fact, precise path following at low speeds and strong lateral stability at high speeds are two contradictory design goals of tractor-trailer wheeled vehicles [5,6]. In low-speed scenarios, the precise path following of a tractor-trailer wheeled vehicle is conducive to obstacle avoidance. In the theoretical analysis of idealized models at low speeds, the lateral speeds of both the tractor and the trailer are assumed to be approximately zero [7,8]. For this reason, a tractor-trailer wheeled structure is regarded as a tractor-trailer wheeled robot (TTWR) in our investigation.

In order to satisfy the path-following requirement for a TTWR, the trailer should be steerable either actively or passively [9]. A TTWR with steerable trailers is called the multi-steering TTWR (MS-TTWR) in [10,11], which has a stronger obstacle

* Corresponding author.
E-mail addresses: yszhou@gzu.edu.cn (Y. Zhou), makchung@cityu.edu.hk (K.-w. Chung).

https://doi.org/10.1016/j.apm.2022.04.025
0307-904X/

avoidance capability and a better steering capability than the one with a passively connected trailer in low-speed scenarios. In [12], a common passive steering mechanism called the rear wheel/axle compliance steering for vehicles is elaborated. The basic principle is that the rear wheel steering can be generated by the lateral force of the rear wheels or the lateral elastic force of a rear suspension. However, the wheel slipping in the case of rear wheel/axle compliance steering may destroy the non-holonomic constraints of zero lateral speed. As described in [13,14], the analysis of motion laws and the establishment of system models would become complicated, which imposes challenges to the model-based controller design.

Another main strategy for steering the trailer is the active axle steering control. As described in the review paper [15], the speed difference of the two rear wheels is generated by steering the rear axle so as to realize the steering of the trailer. It was pointed out in [16] that the tire slipping effect is negligible at low speeds and the non-holonomic constraint of zero lateral speed is retained. Based on the non-holonomic constraints, the required steering speed of the trailer is usually considered as an active control input for the trailer to move along a desired path [17]. In fact, various active control strategies such as the model predictive control [18,19], neural network-based adaptive control [20,21], constrained optimal control [22,23] and adaptive backstepping control [24,25] have been proposed to design speed controllers for the trailer. In this way, the designed speed controllers cannot be directly used in practice since the required speed cannot be achieved instantaneously. Moreover, the control design are usually based on advanced control methods and precise measurement techniques. However, the intrinsic motion laws have not been understood thoroughly and utilized sufficiently. Therefore, the dynamics model of a MS-TTWR is difficult to derive. As a result, the torque controller design mainly focuses on a TTWR with a passively connected trailer. In [26], the speed and torque controllers are designed using the model predictive and adaptive fuzzy control methods, respectively.

To achieve the goal that both the tractor and the trailer follow an identical trajectory curve, the challenging problems include: (i) it is difficult to derive the dynamics equation with steering mechanism; (ii) at least three controllers are needed; (iii) the speed error is accumulated to create a large position error; (iv) the designed controllers are complex and expensive.

Motivated from the above situation, we propose a novel trajectory tracking control strategy for a TTWR based on motion laws. Five aspects of innovations in this paper are described below:

(I) An appropriate passive steering angle achieved by the gear steering mechanism is designed for suitable trailer steering, so that the trailer can follow the motion path of the tractor.

(II) The motion laws of the TTWR with a passive steering angle are established. Then, a standard method is applied to deduce the dynamics equation of the TTWR.

(III) With the aid of the dynamic tracking target, the relative curvature is directly tracked, thereby improving greatly the tracking accuracy of the tractor.

(IV) Only two torque controllers which act on the tractor can provide an effective control of four speed variables.

(V) Both the length of intermediate link and the steering angle coefficient play a significant role on the trajectory of the trailer. Especially when the intermediate link is relatively long, a large magnitude steering angle coefficient is required.

The rest of the paper is organised as follows. In Section 2, the relation between the trajectory curve and the passive steering angle of the trailer is presented. Section 3 establishes the motion laws of the TTWR, followed by a description of the kinematics and dynamics models. In Section 4, an obstacle avoidance motion control problem is discussed. Section 5 presents the trajectory tracking controller design. In Section 6, three simulation examples are considered to illustrate the efficacy of the proposed control strategy. Finally, Section 7 ends with some conclusions.

2. Passive steering angle and gear steering mechanism

Consider a TTWR consisting of a differential-drive tractor and a passive trailer, where a passive spherical wheel is installed on the tractor to keep the balance, as shown in Fig. 1(a). Points Q and P are the midpoints of the two wheels for the trailer and the tractor, respectively. Both the tractor and the trailer are connected flexibly at the end of a rigid intermediate link with on-axle hitching. The related nomenclatures of the TTWR are defined in Table 1. The goal of this study is to design a passive steering angle for the trailer and two appropriate controllers acting on the tractor to compel the trailer and the tractor to track an identical trajectory curve. To this end, in terms of the TTWR, we need the following assumption and definition.

Assumption 1. The TTWR travels at a low speed so that each wheel runs under the conditions of pure rolling and nonslipping.

In this case, all the non-holonomic constraints of the TTWR are not destroyed, and the motion laws can be analyzed theoretically.

Definition 1. The angular difference β between vectors $\overrightarrow{QP}$ and $\overrightarrow{v_0}$ is called a steering angle.

In fact, the steering angle β cannot be too large in practice, otherwise the lateral component force of the drawing force generated by the intermediate link would be large. This would lead to a lateral slip of the trailer, which violates Assumption 1. In theory, if the lateral static friction force of the trailer is large enough, the steering angle β can approach $\pm\frac{\pi}{2}$. Therefore, the range of the steering angle is $\beta \in (-\frac{\pi}{2}, \frac{\pi}{2})$.

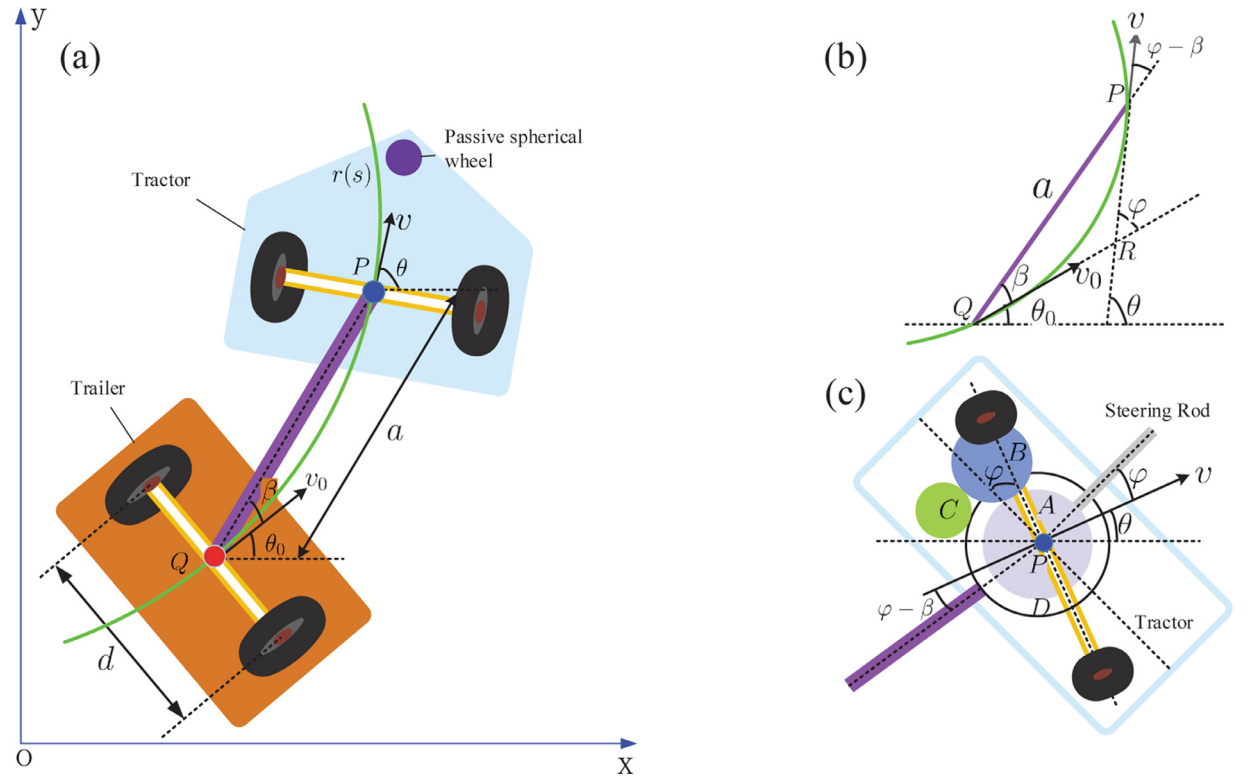

Fig. 1. A TTWR with a passive steering angle: (a) a model of the TTWR, (b) a schematic diagram of the velocity of the intermediate link rod, (c) a gear steering assembly mounted on the tractor.

Table 1
Parameters and variables of the TTWR.

Notation	Unit	Definition
T_l, T_r	N · m	Torques provided by actuators acting on the left and right wheels of the tractor
x, y	m	The coordinates of point P in $X-Y$ plane
x_0, y_0	m	The coordinates of point Q in $X-Y$ plane
θ_l, θ_r	rad	Rotation angles of the left and right wheels of the tractor
θ_{0l}, θ_{0r}	rad	Rotation angles of the left and right wheels of the trailer
θ	rad	Yaw angle of the tractor and $\dot{\theta}=\omega$
θ_0	rad	Yaw angle of the trailer
φ	rad	Angular difference between the yaw angle of the tractor and trailer, and $\varphi=\theta-\theta_0$
β	rad	Steering angle of the trailer
μ		Steering angle coefficient of the steering angle and $\beta=\mu\varphi$
v	m/s	Tangential speed of the center point P of the tractor and $v=\sqrt{\dot{x}^2+\dot{y}^2}$
v_0	m/s	Tangential speed of the center point Q of the trailer
r	m	Radius of the wheel
a	m	Length of the intermediate link
d	m	Distance between the two wheels along the axle center
M_w	kg	Mass of the wheel
M_f	kg	Mass of the tractor without wheels
M_r	kg	Mass of the trailer without wheels
I_{wd}	kg · m^2	Moment of inertia of the wheel about Z-axis through the center of the wheel
I_{fd}	kg · m^2	Moment of inertia of the tractor about Z-axis through the center point P
I_{rd}	kg · m^2	Moment of inertia of the trailer about Z-axis through the center point Q
I_w	kg · m^2	Moment of inertia of the wheel along the wheel axis direction

2.1. Steering angle and target trajectory curve

Assume that both the trailer and the tractor track an identical target trajectory curve $\mathbf{r}(s)$, as depicted in Fig. 1(b). Denote $\mathbf{r}(s)=(x(s),y(s))$ and $\mathbf{r}(s')=(x(s'),y(s'))$ as the coordinate representations of the trailer and the tractor, respectively,

Table 2
The model and control parameters of the TTWR.

Parameter	Nominal value	Parameter	Nominal value
M_w	2 kg	I_w	0.010 kg · m^2
M_f	6 kg	I_{wd}	0.005 kg · m^2
M_r	6 kg	I_{fd}	0.020 kg · m^2
r	0.1 m	I_{rd}	0.020 kg · m^2
d	0.2 m	γ	0.1
ε	0.3	λ	40
ζ	1		

where s and s' stand for arc length parameters. If the length of the intermediate link is a, then one has

$$\mid \mathbf{r}(s') - \mathbf{r}(s) \mid = a. \tag{1}$$

For the target trajectory curve $\mathbf{r}(s)$, since the unit tangent vector at Q is $\dot{\mathbf{r}}(s) = (\dot{x}(s), \dot{y}(s))$, the steering angle $\beta(s)$ is expressed as

$$\cos\beta(s) = \frac{(\mathbf{r}(s') - \mathbf{r}(s)) \cdot \dot{\mathbf{r}}(s)}{a}, \tag{2}$$

where $s = \int_0^t v_0(\tau)\mathrm{d}\tau$ and "$\cdot$" is the dot product. When the TTWR moves along $\mathbf{r}(s)$, the steering angle $\beta(s)$ can be calculated at each point according to Eqs. (1) and (2). In this case, the steering angle $\beta(s)$ is pre-determined, which cannot be adjusted dynamically from time to time. Certainly, it is ideal if both the tractor and the trailer track the same desired path. However, if the actual trajectory of the tractor or the trailer deviates slightly from the target trajectory curve, the deviation will get worse if the above steering angle $\beta(s)$ is adopted.

To solve this problem, the steering angle is designed as the product of a proportional coefficient and the angular difference between the yaw angle of the tractor and that of the trailer, given by

$$\beta(s) := \mu(s)\varphi = \mu(s)(\theta - \theta_0), \tag{3}$$

where $\mu(s)$ is the steering angle coefficient determined by the relative curvature, and φ is the angle between the steering rod and the tangential speed direction of the tractor. Although the steering angle is still a function of the arc length, it is more flexible than the pre-determined one derived from Eqs. (1) and (2). However, the expression of $\mu(s)$ is difficult to identify. Furthermore, it is also difficult to derive the kinematics and dynamics equations, and to implement the design of the steering angle in practice. To fix this issue, we propose a gear steering mechanism to determine the steering angle coefficient $\mu(s)$.

2.2. Gear steering mechanism

Note that the steering angle coefficient $\mu(s)$ in Eq. (3) is a function of the arc length variable, which is difficult to realize in practice. If $\mu(s) \equiv c$ is set to an appropriate constant, a gear steering assembly can be used to achieve the passive steering angle. Fig. 1(c) shows the schematic diagram of the gear steering principle, in which the rotary center axes of wheels A, B, C and D are arranged on the wheel axis of the tractor. The steering rod on the tractor is rigidly connected with gear A, while the traction rod (namely, the intermediate link) of the trailer with gear D. When the steering rod of the tractor swings, the traction rod of the trailer is driven to swing in the opposite direction via the transmission relation of gears A, B, C and D. It is obvious that the gear ratio m of A, B, C and D, which determines the transmission relation between the traction rod and the steering rod, is given by

$$m = \frac{\varphi - \beta}{\varphi}, \qquad m \in (0, +\infty),$$

which yields

$$\beta = (1 - m)\varphi = \mu\varphi, \qquad \mu \in (-\infty, 1). \tag{4}$$

In view of the gear steering assembly, the steering angle coefficient $\mu = 1 - m$ can be implemented by choosing appropriate radii for gears so as to obtain a required passive steering angle. Then, the trailer is able to follow the trajectory of the tractor precisely.

3. Motion laws and system modelling

In this section, we analyze the motion laws, as well as the kinematics and dynamics models of a TTWR in which the passive steering angle is given in Eq. (4).

3.1. Motion laws

From Assumption 1, both the tractor and the trailer satisfy the holonomic constraints

$$\begin{cases}\dot{\theta}_r = \frac{1}{r}v + \frac{d}{2r}\dot{\theta}, \\ \dot{\theta}_l = \frac{1}{r}v - \frac{d}{2r}\dot{\theta}, \end{cases} \qquad \begin{cases}\dot{\theta}_{0r} = \frac{1}{r}v_0 + \frac{d}{2r}\dot{\theta}_0, \\ \dot{\theta}_{0l} = \frac{1}{r}v_0 - \frac{d}{2r}\dot{\theta}_0, \end{cases} \tag{5}$$

and the non-holonomic constraints

$$\begin{cases}-\dot{x}\sin\theta + \dot{y}\cos\theta = 0, \\ v = \dot{x}\cos\theta + \dot{y}\sin\theta, \end{cases} \qquad \begin{cases}-\dot{x}_0\sin\theta_0 + \dot{y}_0\cos\theta_0 = 0, \\ v_0 = \dot{x}_0\cos\theta_0 + \dot{y}_0\sin\theta_0. \end{cases} \tag{6}$$

Since $P(x, y)$ and $Q(x_0, y_0)$ are the end points of the intermediate link, the velocity components are given by

$$\begin{cases}\dot{x} = \dot{x}_0 - a(\dot{\theta}_0 + \dot{\beta})\sin(\theta_0 + \beta), \\ \dot{y} = \dot{y}_0 + a(\dot{\theta}_0 + \dot{\beta})\cos(\theta_0 + \beta). \end{cases} \tag{7}$$

Substituting Eq. (6) into Eq. (7) and eliminating a, one obtains

$$v\cos(\beta - \varphi) = v_0\cos\beta, \tag{8}$$

where $\varphi = \theta - \theta_0$. Substituting Eq. (8) into one of the equations of (7), one obtains

$$\dot{\varphi} = -\frac{\sin\varphi}{a\cos\beta}v + \dot{\theta} + \dot{\beta}.$$

The above analysis is summarised in Theorem 1 which is useful in the motion control design of a TTWR.

Theorem 1. *If Assumption 1 is satisfied, for a given steering angle of a TTWR, the speed of the trailer can be fully derived from that of the tractor, given by*

$$\begin{cases} v_0 = \dfrac{\cos(\beta - \varphi)}{\cos\beta}v, \\ \dot{\varphi} = -\dfrac{\sin\varphi}{a\cos\beta}v + \dot{\theta} + \dot{\beta}. \end{cases} \tag{9}$$

For a known steering angle β and a given initial condition, it follows from Theorem 1 that φ can be determined if $(v, \dot{\theta})$ is provided. Thus, both $\theta_0 = \theta - \varphi$ and v_0 depend on the motion speed of the tractor.

Substituting $\beta = \mu\varphi$ into the second equation of (9), we have

$$\dot{\varphi} = -\frac{\sin\varphi}{a(1-\mu)\cos\beta}v + \frac{1}{1-\mu}\dot{\theta}. \tag{10}$$

Eq. (10) is a crucial non-holonomic constraint which establishes a motion relationship between the trailer and the tractor.

3.2. Kinematics model

Now, we would like to establish the kinematics model of the TTWR by clarifying all the constraint equations under given generalized coordinates. Let $\mathbf{q} := (x, y, \theta, \varphi, \theta_r, \theta_l)^{\mathrm{T}}$ be the generalized coordinates of the TTWR. Eliminating v in Eqs. (5), (6) and (10), all the constraint equations related to $\mathbf{q}$ can be formulated as

$$\begin{cases} -\dot{x}\sin\theta + \dot{y}\cos\theta = 0, \\ \dot{x}\cos\theta + \dot{y}\sin\theta + \frac{d}{2}\dot{\theta} - r\dot{\theta}_r = 0, \\ \dot{x}\cos\theta + \dot{y}\sin\theta - \frac{d}{2}\dot{\theta} - r\dot{\theta}_l = 0, \\ \dot{x}\cos\theta\sin\varphi + \dot{y}\sin\theta\sin\varphi - a\dot{\theta}\cos\beta + a(1-\mu)\dot{\varphi}\cos\beta = 0, \end{cases} \tag{11}$$

which are rewritten in the following matrix form

$$\mathbf{F}(\mathbf{q})\dot{\mathbf{q}} = \mathbf{0}, \tag{12}$$

where

$$\mathbf{F}(\mathbf{q}) = \begin{bmatrix} -\sin\theta & \cos\theta & 0 & 0 & 0 & 0 \\ \cos\theta & \sin\theta & \frac{d}{2} & 0 & -r & 0 \\ \cos\theta & \sin\theta & -\frac{d}{2} & 0 & 0 & -r \\ \cos\theta\sin\varphi & \sin\theta\sin\varphi & -a\cos\beta & a(1-\mu)\cos\beta & 0 & 0 \end{bmatrix}.$$

Defining $\mathbf{V} := (v, \dot{\theta})^{\mathrm{T}}$, it follows again from Eqs. (5), (6) and (10) that

$$\dot{\mathbf{q}} = \mathbf{S}(\mathbf{q})\mathbf{V}, \tag{13}$$

where

$$\mathbf{S}(\mathbf{q}) = \begin{bmatrix} \cos\theta & 0 \\ \sin\theta & 0 \\ 0 & 1 \\ -\frac{\sin\varphi}{a(1-\mu)\cos\beta} & \frac{1}{1-\mu} \\ \frac{1}{r} & \frac{d}{2r} \\ \frac{1}{r} & -\frac{d}{2r} \end{bmatrix}.$$

In fact, Eqs. (12) and (13) are two different forms of the kinematics model of the TTWR with

$$\mathbf{F}(\mathbf{q})\mathbf{S}(\mathbf{q}) = \mathbf{0}.$$

3.3. Dynamics model

Based on the obtained two forms (12) and (13) of the kinematics model, it is convenient to use the Euler-Lagrange equation to deduce its dynamics model. Assume that the mass of the intermediate link is relatively small and negligible.

Then, the kinetic energy of a TTWR is divided into two parts. The first part is the kinetic energy of the tractor which is given by

$$L_f = \tfrac{1}{2}M_w r^2(\dot\theta_r^2 + \dot\theta_l^2) + \tfrac{1}{2}I_w(\dot\theta_r^2 + \dot\theta_l^2) + I_{wd}\dot\theta^2 + \tfrac{1}{2}M_f(\dot x^2 + \dot y^2) + \tfrac{1}{2}I_{fd}\dot\theta^2.$$

With Eq. (8), the second part is the kinetic energy of the trailer which is formulated as

$$L_w = (M_w + \tfrac{I_w}{r^2})[(\dot x^2 + \dot y^2)\tfrac{\cos^2(\varphi-\beta)}{\cos^2\beta} + \tfrac{d^2}{4}(\dot\theta - \dot\varphi)^2] + I_{wd}(\dot\theta - \dot\varphi)^2 + \tfrac{1}{2}M_r(\dot x^2 + \dot y^2)\tfrac{\cos^2(\varphi-\beta)}{\cos^2\beta} + \tfrac{1}{2}I_{rd}(\dot\theta - \dot\varphi)^2.$$

Hence, in accordance with the Euler-Lagrange equation, the dynamics equation of the TTWR is established as

$$\frac{\mathrm{d}}{\mathrm{d}t}\left(\frac{\partial L}{\partial \dot{\mathbf{q}}}\right) - \frac{\partial L}{\partial \mathbf{q}} = \mathbf{E}\mathbf{T} + \mathbf{F}^{\mathrm{T}}(\mathbf{q})\boldsymbol{\lambda}, \tag{14}$$

where $L = L_f + L_w$ is the Lagrangian function and the vector $\boldsymbol{\lambda}$ represents the Lagrange multiplier. $\mathbf{T}$ and $\mathbf{E}$ denote the input torque vector and the control input matrix, respectively, which are given by

$$\mathbf{T} = \begin{pmatrix} T_r \\ T_l \end{pmatrix} \qquad \mathbf{E} = \begin{pmatrix} 0 & 0 & 0 & 0 & 1 & 0 \\ 0 & 0 & 0 & 0 & 0 & 1 \end{pmatrix}^{\mathrm{T}}.$$

Detailed derivations of the related variables in Eq. (14) are given in Appendix A. Then, the dynamics model can be further formulated as

$$\mathbf{A}(\mathbf{q})\ddot{\mathbf{q}} + \mathbf{U}(\mathbf{q}, \dot{\mathbf{q}}) = \mathbf{E}\mathbf{T} + \mathbf{F}^{\mathrm{T}}(\mathbf{q})\boldsymbol{\lambda}, \tag{15}$$

where $\mathbf{A}(\mathbf{q})$ and $\mathbf{U}(\mathbf{q}, \dot{\mathbf{q}})$ are given in Appendix B. Taking the derivative of Eq. (13) with respect to t and noting that $\mathbf{A}(\mathbf{q})$ and $\mathbf{S}^{\mathrm{T}}(\mathbf{q})\mathbf{S}(\mathbf{q})$ are two invertible matrices, we obtain the dynamics equation from Eq. (15) as

$$\dot{\mathbf{V}} = \mathbf{W}^{-1}(\mathbf{q})\mathbf{S}^{\mathrm{T}}(\mathbf{q})\left[\mathbf{E}\mathbf{T} - \mathbf{A}(\mathbf{q})\dot{\mathbf{S}}(\mathbf{q})\mathbf{V} - \mathbf{U}(\mathbf{q}, \dot{\mathbf{q}})\right], \tag{16}$$

where $\mathbf{W}(\mathbf{q}) = \mathbf{S}^{\mathrm{T}}(\mathbf{q})\mathbf{A}(\mathbf{q})\mathbf{S}(\mathbf{q})$.

4. Obstacle avoidance motion control problems

In this section, we consider a motion control problem on obstacle avoidance based on the kinematics and dynamics model of a TTWR. Generally speaking, an obstacle avoidance motion task can be decomposed into a sequence of motion processes. At each motion process, the task is to track accurately an appropriate target trajectory curve. Therefore, in order to design a desired trajectory curve, a set of basic curves should be stored in the intelligent path planning system such as polynomial curves, B-splines and cycloids. During each motion process, the key point is to observe the nearby terrain and the position of the obstacle, and then choose an appropriate parameter curve from the set of basic curves to design an appropriate target trajectory curve.

Assume that the designed target trajectory curve is the green solid line where the parametric expression is $\tilde{\mathbf{r}}(t) = (\tilde x(t), \tilde y(t))$. Then, the controllers T_r and T_l in Eq. (16) with an appropriate steering angle $\beta = \mu\varphi$ are designed so that both the tractor and the trailer track the desired curve $\tilde{\mathbf{r}}(t)$ precisely.

For a given passive steering angle β, it follows from Theorem 1 that v and $\dot\theta$ of the tractor determines both the yaw rotational speed and the tangential speed of the trailer. In other words, under all the constraints of the TTWR, the trajectory of the trailer depends entirely on that of the tractor. Therefore, to achieve an obstacle avoidance motion, the following two steps should be taken into account. First, an appropriate passive steering angle should be designed to make the trailer follow the trajectory of the tractor. According to the analysis in Section 2, the passive steering angle can be adjusted by choosing

appropriate radii of gears. Second, two torque controllers (T_r, T_l) should be designed to make the tractor track the desired trajectory accurately.

For the tractor tracking the desired trajectory accurately, we have to combine the target trajectory curve $\tilde{\mathbf{r}}(t)$ with the dynamics Eq. (16). Note that the dynamics Eq. (16) is concerned with the yaw rotational speed and the tangential speed of the tractor. It is difficult to directly combine the dynamics equation with the given target trajectory curve. Thus, in order to match the dynamics Eq. (16) as in [27], we make good use of the curvature $k(t)$ of the target trajectory curve $\tilde{\mathbf{r}}(t)$ where $k(t) = \frac{\dot{\tilde{x}}\ddot{\tilde{y}} - \ddot{\tilde{x}}\dot{\tilde{y}}}{(\dot{\tilde{x}}^2 + \dot{\tilde{y}}^2)^{\frac{3}{2}}}$. Thus, we have

$$\tilde{\mathbf{V}} = \begin{pmatrix} \tilde{v} \\ \tilde{\omega} \end{pmatrix} = \begin{pmatrix} \sqrt{\dot{\tilde{x}}^2 + \dot{\tilde{y}}^2} \\ k(t)\tilde{v} \end{pmatrix}.$$

On the other hand, the target curve $\tilde{\mathbf{r}}(t)$ can also be expressed in a dynamic speed form as

$$\tilde{\mathbf{V}} = \begin{pmatrix} \dot{\phi}(t) \\ k(s)v \end{pmatrix}, \tag{17}$$

where $\dot{\phi}(t)$ is an arbitrary smooth function designed to cater for actual needs, and $s = \int_0^t v(\tau)\mathrm{d}\tau$ with $v(t)$ being the actual tangential speed of the tractor. In this way, by combining Eqs. (16) with (17), the original motion task is reduced to an ordinary tracking control problem. In addition, as long as the curvature function $k(s)$ is well tracked, the target trajectory curve can be tracked precisely. From the above analysis, we only need to design two torque controllers (T_r, T_l) for the tractor to track the desired curve accurately via the dynamic tracking target (17).

5. Trajectory tracking control design

In this section, we first design two torque controllers for the dynamics Eq. (16) via the dynamic tracking target (17) in order that the tractor is able to track a target trajectory curve closely. Then, we analyze the implementation and efficiency of the designed torque controllers.

5.1. Torque controllers design

At first, a feedback linearization method is adopted to Eq. (16). Define $\mathbf{H} = (h_1, h_2)^{\mathrm{T}}$ as

$$\mathbf{H} = \mathbf{W}^{-1}(\mathbf{q})\mathbf{S}^{\mathrm{T}}(\mathbf{q})\big[\mathbf{ET} - \mathbf{A}(\mathbf{q})\dot{\mathbf{S}}(\mathbf{q})\mathbf{V} - \mathbf{U}(\mathbf{q}, \dot{\mathbf{q}})\big], \tag{18}$$

so that Eq. (16) is expressed in the following simple form

$$\dot{\mathbf{V}} = \mathbf{H}. \tag{19}$$

We note that $\tilde{\omega}$ in the second equation of (17) contains the actual tangential speed v. With regard to Eq. (19), the tangential motion subsystem should be considered first, followed by the yaw motion subsystem. To this end, we set $\mathbf{X} = (s, v)^{\mathrm{T}}$ with $s = \int_0^t v(\tau)\mathrm{d}\tau$. Then the tangential motion subsystem is rewritten as

$$\dot{\mathbf{X}} = \mathbf{A}\mathbf{X} + \mathbf{B}h_1, \tag{20}$$

where $\mathbf{A} = \begin{pmatrix} 0 & 1 \\ 0 & 0 \end{pmatrix}$ and $\mathbf{B} = \begin{pmatrix} 0 \\ 1 \end{pmatrix}$. The tracking target of Eq. (20) is presented as $\tilde{\mathbf{X}} = (\tilde{s}, \tilde{v})^{\mathrm{T}}$ with $\tilde{s} = \int_0^t \tilde{v}(\tau)\mathrm{d}\tau$. Then, the error of the tangential motion subsystem relative to the tracking target, $\boldsymbol{\Delta}\mathbf{X} = \mathbf{X} - \tilde{\mathbf{X}}$, satisfies the following system of equations

$$\boldsymbol{\Delta}\dot{\mathbf{X}} = \mathbf{A}\boldsymbol{\Delta}\mathbf{X} + \mathbf{B}h_1 + \boldsymbol{\eta}, \tag{21}$$

where $\boldsymbol{\eta} = \mathbf{A}\tilde{\mathbf{X}} - \dot{\tilde{\mathbf{X}}}$. To improve the accuracy of trajectory tracking, we need to choose a tangential speed target for actural requirements and a performance index for achieving optimal control. In general practical problems, a TTWR is at rest in the beginning and at the end of a trajectory. Thus, an appropriate tangential speed target $\dot{\phi}(t)$ should be designed such that the initial and the terminal speed errors equal to zero. For example, a simple tangential speed target can be designed as

$$\dot{\phi}(t) = l\alpha^2 t\mathrm{e}^{-\alpha t}, \tag{22}$$

where α represents a tunable parameter and l denotes the arc length of the desired path [27]. Since the integral of the tangential speed target (22) over time from 0 to infinity converges, it is reasonable to introduce the linear quadratic performance index as follows

$$J = \frac{1}{2}\int_0^{\infty} (\boldsymbol{\Delta}\mathbf{X}^{\mathrm{T}}\mathbf{Q}\boldsymbol{\Delta}\mathbf{X} + w_c h_1^2)\mathrm{d}t, \tag{23}$$

where the positive definite symmetric matrix $\mathbf{Q}$ has a large weight on the tangential speed error and w_c is the weight of the controller h_1. To minimize the performance index (23), the optimal control ensures that the tangential speed error is small enough throughout the entire trajectory. Based on the linear quadratic regulator method, h_1 is expressed by

$$h_1 = -\frac{1}{w_c}\mathbf{B}^{\mathrm{T}}(\mathbf{P}\boldsymbol{\Delta}\mathbf{X} + \mathbf{b}), \tag{24}$$

where $\mathbf{P} \in \mathbb{R}^{2\times 2}$ and $\mathbf{b} \in \mathbb{R}^{2\times 1}$ are given by

$$\begin{cases} -\mathbf{P}\mathbf{A} - \mathbf{A}^{\mathrm{T}}\mathbf{P} + \frac{1}{w_c}\mathbf{P}\mathbf{B}\mathbf{B}^{\mathrm{T}}\mathbf{P} - \mathbf{Q} = \mathbf{0}, \\ \dot{\mathbf{b}} = -(\mathbf{A} - \frac{1}{w_c}\mathbf{B}\mathbf{B}^{\mathrm{T}}\mathbf{P})^{\mathrm{T}}\mathbf{b} - \mathbf{P}\boldsymbol{\eta}, \quad \mathbf{b}(+\infty) = \mathbf{0}. \end{cases}$$

We now consider the yaw motion subsystem of (19) by using the obtained actual tangential speed v. Define the error of the yaw rotational speed as $e := \omega - \tilde{\omega}$. It follows from Eq. (19) that

$$\dot{e} = h_2 - \dot{\tilde{\omega}}.$$

To improve the robustness of trajectory tracking, we apply the integral sliding mode control to the yaw motion subsystem. At first, the basic part h_{20} is expressed by

$$h_{20} = -\lambda e + \dot{\tilde{\omega}}, \tag{25}$$

where λ represents an appropriate gain parameter. Define the sliding mode function $S(\omega(t))$ as

$$S(\omega(t)) := \zeta[\omega(t) - \omega(0)] - \zeta\int_0^t \dot{\tilde{\omega}}(\eta)\mathrm{d}\eta,$$

with $\zeta > 0$ being an appropriate constant. Then, $\tilde{\omega}$ is designed as the integral sliding manifold which satisfies $S(\tilde{\omega}) = 0$. Therefore, the switching control part h_{21} is expressed by

$$h_{21} = (-\frac{\gamma}{\zeta} - \varepsilon|e|)\mathrm{sgn}(S(\omega(t))), \tag{26}$$

where $\gamma > 0$ and $\varepsilon > 0$ stand for appropriate control parameters. Finally, from Eqs. (25) and (26), h_2 is eventually designed as

$$h_2 = h_{20} + h_{21}. \tag{27}$$

Substituting Eqs. (24) and (27) into Eq. (18), we obtain the desired controllers T_r and T_l in $\mathbf{T}$ as

$$\mathbf{T} = \mathbf{A_1}\left[\mathbf{W}(\mathbf{q})\mathbf{H} + \mathbf{S}^{\mathrm{T}}(\mathbf{q})\mathbf{A}(\mathbf{q})\dot{\mathbf{S}}(\mathbf{q})\mathbf{V} + \mathbf{S}^{\mathrm{T}}(\mathbf{q})\mathbf{U}(\mathbf{q},\dot{\mathbf{q}})\right], \tag{28}$$

where $\mathbf{A_1} = \left[\mathbf{S}^{\mathrm{T}}(\mathbf{q})\mathrm{E}\right]^{-1} = \begin{pmatrix} \frac{r}{2} & \frac{r}{d} \\ \frac{r}{2} & -\frac{r}{d} \end{pmatrix}$. Both φ and $\beta = \mu\varphi$ in T_r and T_l are determined by Eq. (10).

5.2. Implementation of controllers

Substituting the designed controllers (28) into the dynamics Eq. (16) together with Eq. (10), we obtain the following three-dimensional nonlinear system

$$\begin{cases} \dot{v} = f(v,\omega,\varphi), \\ \dot{\omega} = g(v,\omega,\varphi), \\ \dot{\varphi} = -\frac{\sin\varphi}{a(1-\mu)\cos\beta}v + \frac{1}{1-\mu}\omega, \end{cases} \tag{29}$$

where f and g are nonlinear functions. According to the analysis of the dynamic tracking target (17) in Section 4, the essence of applying the dynamic tracking target is to track the relative curvature of the target curve from the tractor, thereby achieving accurate trajectory tracking. Regarding the trailer, since $\theta_0 = \theta - \varphi$, a relation between (v_0, ω_0) and (v, ω) is obtained from Eqs. (8) and (10) as

$$\begin{cases} v_0 = -\frac{\cos(\beta-\varphi)}{\cos\beta}v, \\ \omega_0 = \frac{\sin\varphi}{a(1-\mu)\cos\beta}v - \frac{\mu}{1-\mu}\omega. \end{cases} \tag{30}$$

We note that the design of the control torques T_r and T_l is to well track the dynamic tracking target (17) using v and ω in system (29). It follows from Eq. (30) that v_0 and ω_0 also depend on the controllers T_r and T_l. Moreover, μ in the passive steering angle $\beta = \mu\varphi$ is an appropriate parameter obtained by the gear steering assembly given in Fig. 1(c), such that the trailer follows well the trajectory of the tractor. From the above analysis, the four speed variables v, ω, v_0 and ω_0 can be controlled by only two active control torques T_r and T_l owing to the introduction of μ in $\beta = \mu\varphi$. Compared with many existing studies [9,15], the proposed control method requires relatively fewer state inputs. This results in less control components and thus energy loss is reduced. From this perspective, the proposed method has the advantage of low energy consumption and easy implementation.

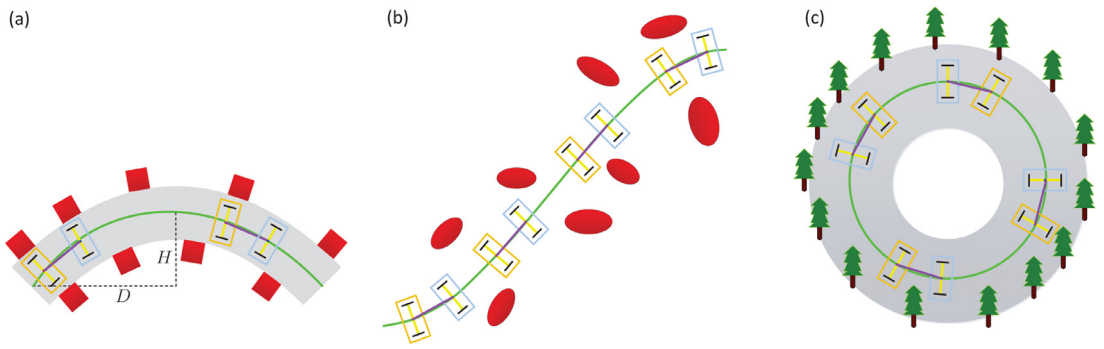

Fig. 2. Schematic diagram of the obstacle avoidance motion control problems in which the target trajectory curve is (a) a cycloid, (b) a polynomial curve, (c) a circle.

5.3. Efficiency of controllers

As the ultimate goal of the two active controllers is to assure that the tractor follows well a given target trajectory curve, it is not important whether the tangential speed target is tracked accurately or not. The major role of tracking the tangential speed target is to generate a forward motion of the tractor. In Section 5.1, the linear quadratic optimal control method is adopted to design a state-feedback controller for the tractor to track the tangential speed target. In this way, the weight matrix in the performance index J of (23) can be adjusted to satisfy the actual motion requirements. Furthermore, to ensure the robustness of curvature tracking, the integral sliding mode controller (27) is adopted for the tractor to track the yaw rotational speed target in Eq. (17).

We now consider the efficiency of the integral sliding mode controller (27). Let $V = \frac{1}{2}S^2(\omega(t))$ be a Lyapunov function for the yaw rotational speed subsystem. Taking the derivative of V with respect to t, we have, from Eqs. (25)–(27),

$$\begin{aligned}\frac{\mathrm{d}V}{\mathrm{d}t} &= \zeta S(\dot{\omega} - \dot{\tilde{\omega}})\\ &= \zeta S(h_{20} + h_{21} - \dot{\tilde{\omega}})\\ &= -\zeta S\lambda e - \gamma|s| - \zeta\varepsilon|e|\cdot|s|\\ &= -\zeta^2\lambda(\omega - \tilde{\omega})^2 - \gamma|s| - \zeta\varepsilon|e|\cdot|s| < 0,\end{aligned}$$

where $\tilde{\omega}(0) = \omega(0)$. Thus, the proposed sliding mode controller is effective.

Since the integral sliding mode control is strong in robustness, it can keep the yaw rotational speed error $e = \omega - \tilde{\omega}$ within a limited range. Using the proposed integral sliding mode control (27), the curvature tracking error $|K_e|$ can be calculated as

$$|K_e| = \left|\frac{\omega}{v} - k(s)\right| = \frac{|\omega - \tilde{\omega}|}{v} = \frac{|e|}{v}. \tag{31}$$

It can be seen from Eq. (31) that although the linear quadratic optimal control method would lead to poor robustness for the tangential motion subsystem, the large tangential speed error does not affect the curvature tracking error $|K_e|$, i.e. the tracking precision of the target trajectory curve for the tractor. If the actual tangential speed is small, it will not result in a large $|K_e|$. This is because the yaw rotational speed target $\tilde{\omega} = k(s)v$ is also small, and appropriate sliding control parameters γ and ε can be selected to make the corresponding yaw rotational speed error smaller. As long as the actual tangential speed is not zero during the journey, the tracking accuracy of the tractor to the target curve can be guaranteed. From the analysis in Section 2, the trailer can track well the trajectory of the tractor by means of a proper passive steering angle. As a result, all bodies are able to move along the desired path accurately and so the proposed torque controllers given in Eq. (28) are effective.

6. Simulation results

In this section, we present three examples as depicted in Fig. 2 to illustrate the effectiveness of the proposed control strategy.

6.1. Obstacle avoidance motion control on a cycloid

The first example that we would like to consider is an obstacle avoidance motion control problem as depicted in Fig. 2(a). The target trajectory $\tilde{\mathbf{r}}(t)$ is modelled by a cycloid with the following parametric expression

$$\tilde{\mathbf{r}}(t) = (c_1[c_2t + c_3 - \sin(c_2t + c_3)],\ c_1[1 - \cos(c_2t + c_3)]),\quad t \in \left[0, \tfrac{2\pi - 2c_3}{c_2}\right], \tag{32}$$

where c_1, c_2, c_3 are parameters. Note that the adopted dynamic tracking target (17) is mainly concerned with the accurate tracking of the path curve, rather than the motion speed in the tracking process. As c_2 affects the motion speed only, we

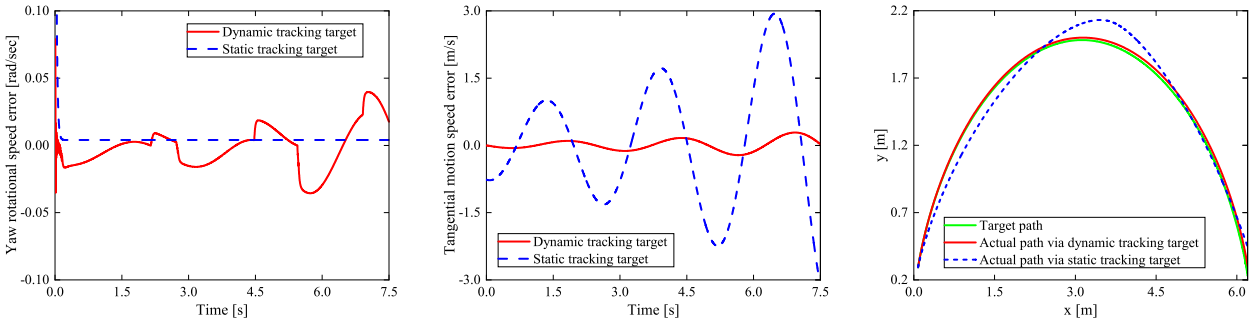

(a) Yaw rotational speed error (b) tangential speed error (c) Actual motion trajectory

Fig. 3. Actual motion trajectory of the tractor with $\boldsymbol{d} = \boldsymbol{d}_1$ for the target trajectory curve $\tilde{\mathbf{r}}(t)$ defined in (34)

assume $c_2 = 1$ without loss of generality. Let D be half of the total horizontal distance travelled and H be the maximum height of the cycloid. It follows from Eq. (32) for $t \in \{0, \pi - c_3, 2(\pi - c_3)\}$ that

$$\begin{cases} c_1(\pi - c_3 + \sin c_3) = D, \\ c_1(1 + \cos c_3) = H, \end{cases} \tag{33}$$

from which c_1 and c_3 can be determined if D and H are given. For a practical obstacle avoidance application, one can roughly design appropriate values of D and H according to the actual need, and then calculate the unknown parameters c_1 and c_3 using Eq. (33). From this point of view, the parameter curve (32) is useful in the design of appropriate target curves for obstacle avoidance motion problems.

By using suitable coordinate transformation, we may let $c_1 = 1$ and $c_3 = \frac{\pi}{4}$. Eq. (32) becomes

$$\tilde{\mathbf{r}}(t) = (t + \frac{\pi}{4} - \sin(t + \frac{\pi}{4}), 1 - \cos(t + \frac{\pi}{4})), \qquad t \in \left[0, \frac{3}{2}\pi\right]. \tag{34}$$

On the one hand, the trajectory curve (34) can be transformed into a static speed target form as follows

$$\begin{cases} \tilde{v} = \sqrt{\dot{\tilde{x}}^2 + \dot{\tilde{y}}^2} = 2\sin(\frac{t+\frac{\pi}{4}}{2}), \\ \dot{\tilde{\theta}} = \frac{\dot{\tilde{x}}\ddot{\tilde{y}} - \ddot{\tilde{x}}\dot{\tilde{y}}}{\dot{\tilde{x}}^2 + \dot{\tilde{y}}^2} = -\frac{1}{2}. \end{cases} \tag{35}$$

On the other hand, the corresponding arc length and curvature function of the target curve (34) are expressed as, respectively,

$$\begin{aligned} s &= \int_0^t \sqrt{2(1 - \cos(\tau + \tfrac{\pi}{4}))}\mathrm{d}\tau = 4\cos\tfrac{\pi}{8} - 4\cos(\tfrac{t}{2} + \tfrac{\pi}{8}), \\ k(s) &= -\frac{1}{\sqrt{16 - 16\cos^2\frac{\pi}{8} - s^2 + 8s\cos\frac{\pi}{8}}}. \end{aligned}$$

Therefore, from Eq. (17), the dynamic tracking target is designed as

$$\begin{cases} \tilde{v} = 2te^{-\frac{1}{2}t}, \\ \tilde{\omega} = k(s)v, \qquad s \in [0, 8\cos\frac{\pi}{8}). \end{cases} \tag{36}$$

In fact, Eqs. (35) and (36) indicate two different speed forms of the trajectory curve (34). The static speed target (35) is in an open loop form, while the dynamic tracking target (36) is in a closed loop form.

The model and control parameters of the TTWR are presented in Table 2. Accordingly, the related initial values are set as $\dot{x}(0) = \dot{y}(0) = 0$, $\theta(0) = \frac{3}{8}\pi$. It should be noted that, for the trajectory tracking control design in Section 5, the control design of (21) is based on the optimal control theory which has poor robustness, while the yaw motion subsystem is controlled by an integral sliding mode controller which has strong robustness. Thus, to verify the impact of uncertainties on the tracking performance, we assume that the tangential motion error subsystem is affected by various uncertainties. Then, for an uncertainty $\boldsymbol{d}$, the system (21) becomes

$$\boldsymbol{\Delta}\dot{\mathbf{X}} = \mathbf{A}\boldsymbol{\Delta}\mathbf{X} + \mathbf{B}h_1 + \boldsymbol{\eta} + \boldsymbol{d}. \tag{37}$$

Now, we compare the tracking effect of the tractor with dynamic tracking target (36) and static tracking target (35) under different uncertainties. We first consider the uncertainty $\boldsymbol{d} = \boldsymbol{d}_1 = (5(s - \tilde{s}),\ 10.5(v - \tilde{v}))^{\mathrm{T}}$ which depends on the error states. By exploiting the dynamic tracking target (36) and the controllers (28), we find that both the yaw rotational speed error and the tangential speed error of the tractor become arbitrarily large as time goes by (see the red solid line in Fig. 3(a) and (b)). However, the trajectory of the tractor coincides nearly with the target curve (34) via tracking its relative curvature, as shown in Fig. 3(c). This indicates that it can achieve accurate tracking of the target path as well as with strong robustness via the dynamic tracking target. On the contrary, by using the static tracking target, although the yaw rotational speed error

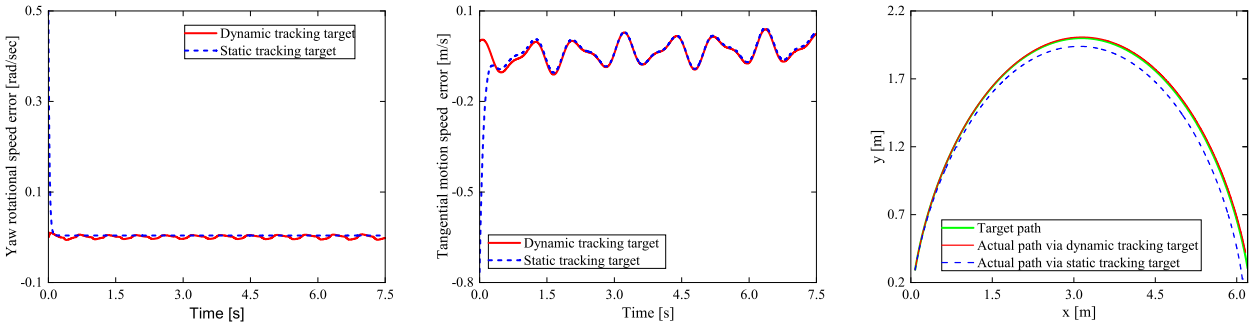

(a) Yaw rotational speed error (b) tangential speed error (c) Actual motion trajectory

Fig. 4. Actual motion trajectory of the tractor with $\boldsymbol{d} = \boldsymbol{d}_2$ for the target trajectory curve $\tilde{\mathbf{r}}(t)$ defined in (34)

is relatively small, the tangential speed error is too large, as reflected in the blue dashed line in Fig. 3(a) and (b). This makes the ratio of the actual yaw rotational speed to the actual tangential speed deviate significantly from the curvature value of the target path. Consequently, in the blue dashed line in Fig. 3(c), the actual motion path of the tractor deviates from the target path.

Next, we consider an external periodic disturbance of $\boldsymbol{d} = \boldsymbol{d}_2 = (0.2\sin t,\ 0.4\cos t)^{\mathrm{T}}$ which is time varying but independent of the error states. As depicted in Fig. 4(b), the tangential speed error is bounded with the similar frequency as the external disturbance. Because of adopting the dynamic tracking target, the yaw rotational speed error is affected by the tangential speed error, as shown in Fig. 4(a), where the frequency is almost consistent with that of the tangential speed error. In this case, the ratio of the actual yaw rotational speed to the actual tangential speed is relatively closed to the relative curvature of the target path. Thus, satisfactory tracking performance for the tractor can be achieved, as shown in Fig. 4(c). However, if the static target is adopted, the yaw rotational speed error is independent of the tangential speed error. Therefore, the yaw rotational speed does not change accordingly with the tangential speed. This results in a deviation of the ratio of the actual yaw rotational speed to the actual tangential speed from its relative curvature, causing the tractor to deviate from the target path.

The above two examples show that accurate trajectory tracking of the tractor with strong robustness can be achieved even though the yaw rotational speed and the tangential speed errors may be large. In essence, the tracking of relative curvature of the target curve plays a significant role in this dynamic tracking target approach. As long as the error between the ratio of the actual yaw rotational speed to the tangential speed and the relative curvature of the target curve is small enough, the tracking precision obtained using the proposed control strategy can be guaranteed even if the speed error is large.

In what follows, we take into account the actual tracking effect of the trailer. According to Theorem 1, the speed of the trailer is significantly affected by the length of the intermediate link a and the steering angle coefficient μ. Therefore, we analyze the influence of these two factors on the actual path of the trailer if the tractor follows the target path accurately. We start with a small intermediate link length such as $a = 0.2$m and investigate the tracking effect of the trailer for different values of the steering angle coefficient such as $\mu = 0, 0.8, -4.0$ and -8.0. When the steering angle is zero, i.e. $\mu = 0$, the actual path of the trailer can follow really well with the target path as represented by the purple dashed line in Fig. 5(a). For $\mu = 0.8$, the actual path of the trailer deviates to the left side of target path as represented by the blue dashed line. If the steering angle coefficient is negative with a relatively large magnitude such as $\mu = -4.0$ or -8.0, the actual path of the trailer drifts to the right side of the target path, as depicted in Fig. 5(b).

For a longer intermediate link length $a = 0.4$m, the tracking effect of the trailer for the steering angle coefficients $\mu = 0, 0.8$ and $\mu = -4.0, -5.6$ are depicted in Fig. 6(a) and (b), respectively. Comparing Figs. 5(a) and 6(a), for positive μ, the tracking performance of actual path of the trailer is poorer when a increases and the drift to the left increases with μ. However, for negative μ, the tracking effect of the trailer is the best at round $\mu = -5.6$ as represented by the purple dashed line in Fig. 6(b).

The above analysis shows that both the length of the intermediate link and the steering angle coefficient indeed play a significant role in the motion trajectory of the trailer. Therefore, an appropriate parameter pair (a, μ) can be selected to achieve an optimal actual path of the trailer.

To further verify the influence of the length of intermediate link and the steering angle coefficient on the trajectory curve error of the trailer, we would like to calculate the sum of the square errors between the actual path of the trailer and the target trajectory curve. Let h be a step length and $M = hN$ where $N \in \mathbb{I}^+$. Let $(x_r(k), y_r(k))$ be the coordinate of the actual path of the trailer at $x_r(k) = kh$ and $0 \le k \le N$. For the same abscissa $x_r(k)$, let $(x_r(k), \hat{y}_r(k))$ be the corresponding point on the target trajectory curve. It follows from Eq. (34) that

$$x_r(k) = kh = t_k + \frac{\pi}{4} + \sin(t_k + \frac{\pi}{4}), \quad \hat{y}_r(k) = 1 - \cos(t_k + \frac{\pi}{4}).$$

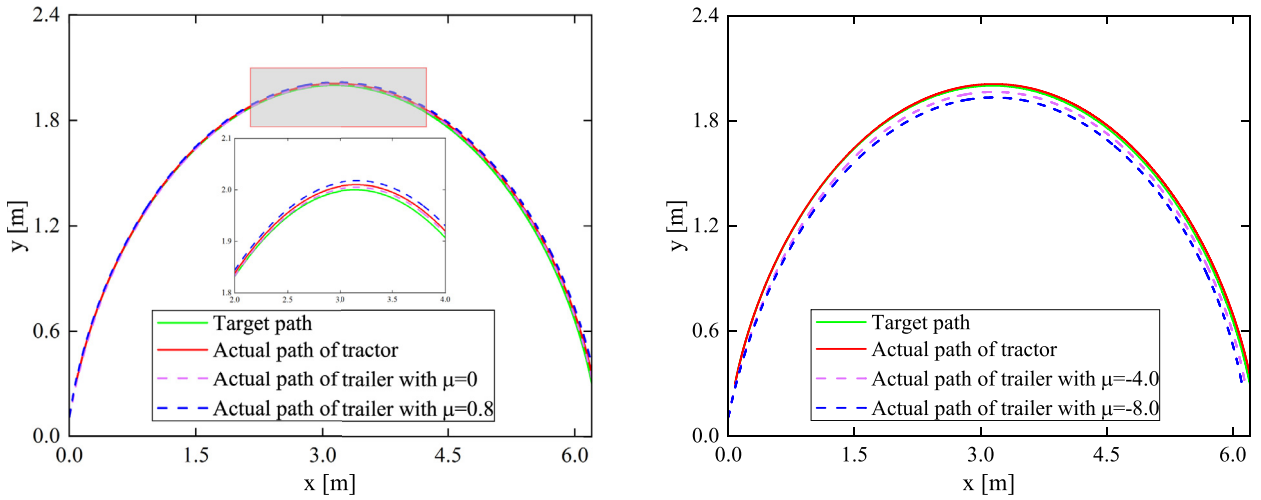

Fig. 5. Actual motion trajectories of the trailer under different steering angle coefficients at $a = 0.2$m.

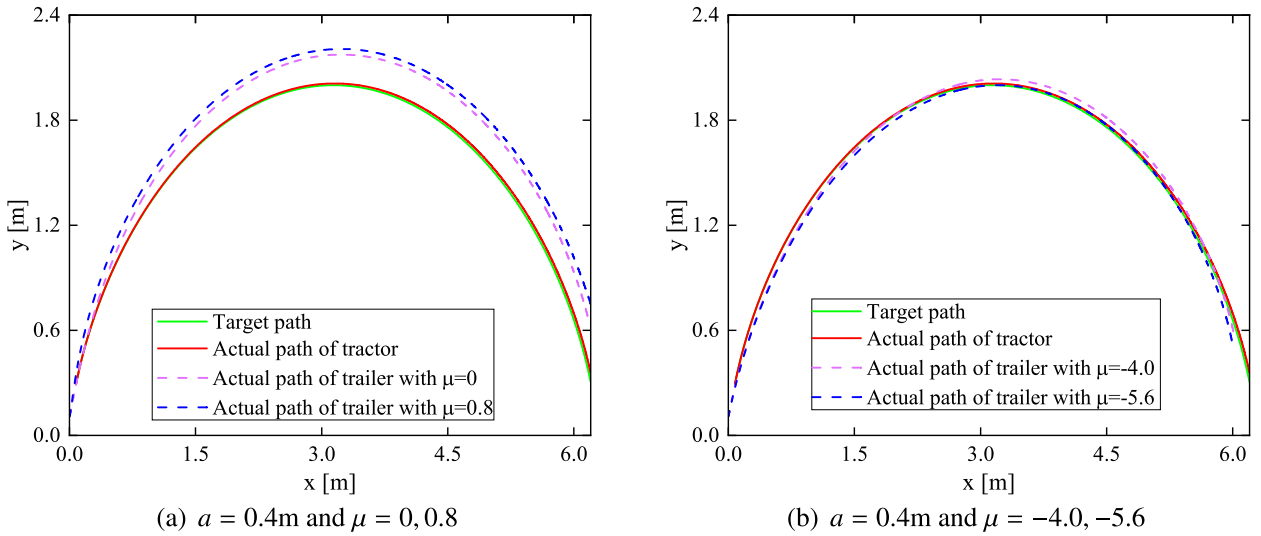

Fig. 6. Actual motion trajectories of the trailer under different steering angle coefficients at $a = 0.4$m.

Given h and k, t_k and $\hat{y}_r(k)$ can be found numerically. The square error of point $(x_r(k), y_r(k))$ is denoted by $(\hat{y}_r(k) - y_r(k))^2$. Then, the sum of the squared errors J_r of the actual trajectory curve is expressed as

$$J_r = \sum_{k=1}^{N} (y_r(k) - \hat{y}_r(k))^2. \tag{38}$$

We choose $h = 0.0001$ and $N = 62,000$ for the error analysis. The contours of the trajectory error obtained from Eq. (38) for the region of $\mu \in [-8.0, 0.8]$ and $a \in [0.2, 0.8]$ is depicted in Fig. 7. In the case of a small intermediate link length, satisfactory tracking performance can be achieved only with a small steering angle coefficient. On the other hand, with a large intermediate link length, a negative steering angle coefficient with large magnitude should be used to minimize the trajectory curve error of the trailer.

6.2. The case of a polynomial curve

In this subsection, we focus on the case of a polynomial curve as depicted in Fig. 2(b). As a comparison, we consider the curve investigated in Section 5.1 of [11]. The length of intermediate link was chosen as $a = 1.0$m and the target trajectory curve was expressed in a vector form as $\hat{\mathbf{r}}(t) = (t, 0.3t^2 - 0.02t^3)$ where $t \in [0, 10]$. The parameters

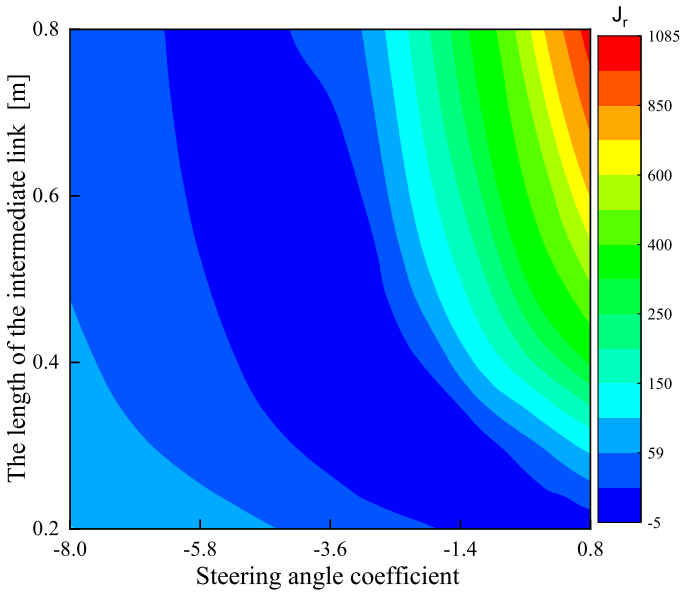

Fig. 7. Contours of the trajectory curve error J_r of the trailer in the (μ, a)-plane.

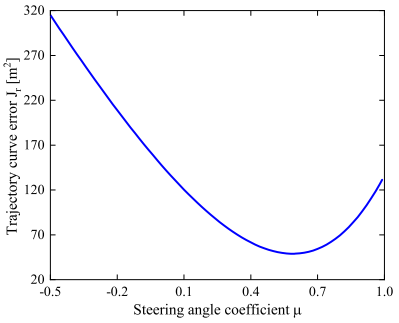

(a) The trajectory curve error of the trailer under different steering angle coefficients

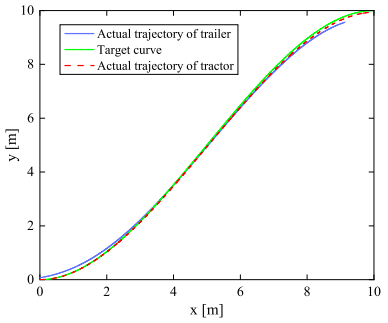

(b) Actual motion trajectories with $\mu = 0$

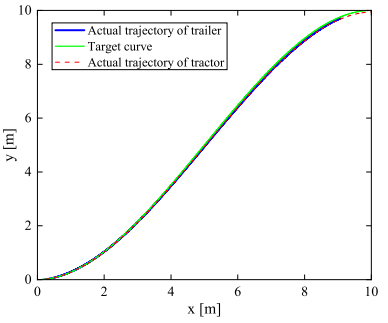

(c) Actual motion trajectories with $\mu = 0.6$

Fig. 8. Actual motion trajectories of the TTWR for the target trajectory curve $y = 0.3x^2 - 0.02x^3$.

$M_w, M_f, M_r, r, d, T_w, I_{wd}, I_{fd}$ and I_{rd} of the tractor and the trailer are given in Table 2. The controller parameters are set to be $\varepsilon = 0.2, \lambda = 10$ and $\zeta = 1$. As the steering angle coefficient μ varies, the actual trajectory curve error (38) obtained with $h = 0.0001$ and $N = 100000$ is shown in Fig. 8(a). A minimum trajectory curve error is achieved at around $\mu = 0.6$. The actual trajectories of the tractor and the trailer for $\mu = 0$ and $\mu = 0.6$ with $a = 1.0$m are shown in Fig. 8(b) and (c), respectively. Note that there is little difference in the tracking performance between the results in Fig. 8(c) of this paper and Fig. 4(a) of [11]. However, the present method has the following two advantages: (i) the design of the two torque controllers is more in line with the actual situation than that of the speed controllers which considers the kinematics equation only, and (ii) the steering motion of the trailer from the present method is achieved by a passive steering angle and its steering mechanism. As a result, the controllers are simple to design, easy to implement and at a low cost.

6.3. The case of a circle discussed in [28]

In this subsection, we comment on the relation between the steering strategy presented in this paper and that in [28]. According to the motion laws of the TTWR with a passively connected trailer investigated in [28], it is impossible to apply only two driven torques on the tractor so that both the tractor and the trailer follow an identical target trajectory curve. To solve this problem, a passive steering angle and its gear steering mechanism for the trailer are proposed in this paper. In theory, the model in [28] can be regarded as the special case of $\beta = 0$ in the proposed control strategy.

In the simulation example of [28], since the desired trajectory of the tractor is a circle, we have $|QR| = |PR|$ as shown in Fig. 1(b). Then, the steering angle is given by $\beta = 0.5\varphi$, thereby $\mu = 0.5$. As shown in Fig. 9(a), without adopting any steering angle, i.e. $\mu = 0$, the motion trajectory of the trailer in [28] is a unit circle, while the actual trajectory of the tractor

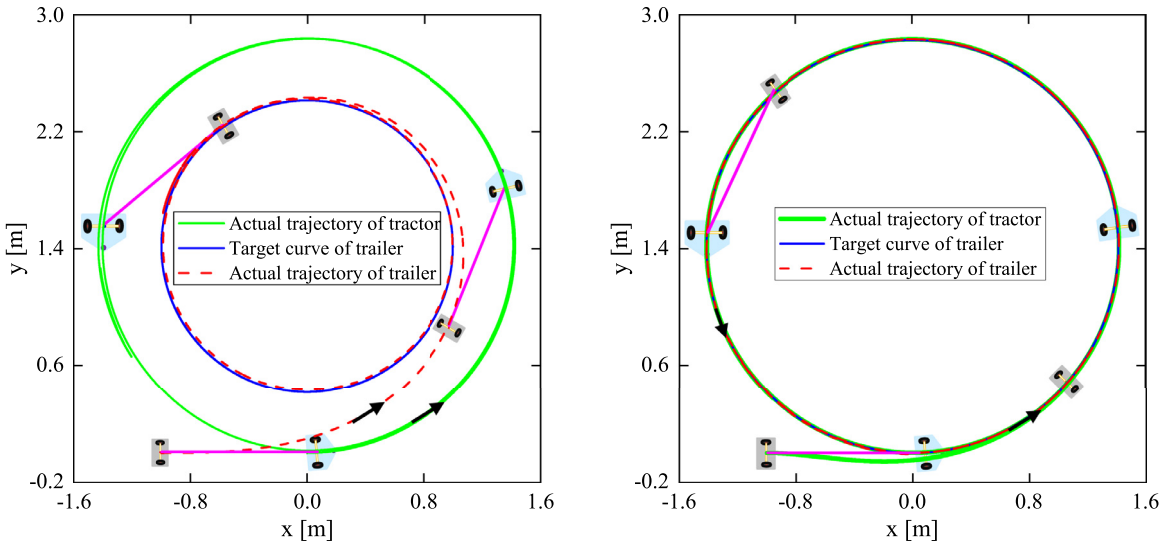

(a) Without steering angle in [28] (b) With steering angle $\beta = \frac{1}{2}\varphi$

Fig. 9. Actual motion trajectories of the TTWR for the target trajectory of a circle with radius $\sqrt{2}$.

is a circle with radius $\sqrt{2}$. The tractor and the trailer follow two different target curves. However, when the steering angle coefficient $\mu = 0.5$ is adopted, the motion trajectories of both the tractor and the trailer follow the same circle with radius $\sqrt{2}$ as depicted in Fig. 9(b). Therefore, both the tractor and the trailer move along an identical path simultaneously, provided that the length of the intermediate link is less than the radius of the circle.

7. Conclusions and future work

For a tractor-trailer wheeled robot (TTWR), a novel trajectory tracking control strategy is proposed to achieve the goal that both the tractor and the trailer move along an identical trajectory curve precisely. Different from most control strategies discussed in the current literature, an appropriate passive steering angle as well as its steering mechanism for the trailer is introduced so that the trailer can follow well the motion path of the tractor. Most importantly, the motion laws of the TTWR with a passive steering angle are clarified and utilized fully for designing torque controllers. In this way, without using advanced control methods or accurate measurement techniques, only two torque controllers designed by the integral sliding mode control and the linear quadratic regulator can readily achieve the goal. Moreover, since the relative curvature is directly tracked via a dynamic tracking target, tracking precision of the target path can be guaranteed for the tractor even when the error of tracking speed is large.

The proposed strategy is applied to the obstacle avoidance motion problem of three different target trajectories, namely a cycloid, a polynomial curve and a circle. Simulation results show that tracking the relative curvature directly improves greatly the tracking accuracy. Furthermore, choosing an appropriate steering angle coefficient can reduce dramatically the deviation of the trailer from the target curve even though the length of the intermediate link is large. Therefore, the proposed control strategy can be applied to overcome the challenging problems addressed in the Introduction. The two controllers are simple to design, easy to implement and the cost is low as well.

From Assumption 1, a TTWR travelling at a low speed is subjected to all non-holonomic constraints described in Section 3. However, if the travelling speed is not low, the lateral slipping of wheels would be inevitable when it goes round a bend. In this case, the motion law given in Theorem 1 is no longer effective. One of our future investigations will be on the compensation of the influence of lateral slipping of wheels in the control design. This will extend our investigation to the path tracking control of tractor-trailer systems which travel at an arbitrary speed.

The passive steering angle coefficient proposed in this control strategy is difficult to find directly for a prescribed target trajectory curve. Thus, an appropriate steering angle coefficient is obtained by means of a parameter tuning. From a practical point of view, the proposed passive steering angle has a potential application in the implementation of motion tasks of multiple mechanical structures which are connected among one another. Furthermore, if the travelling speed is arbitrary, then the curvature tracking method may be extended to path tracking control problems in the three-dimensional space. This is the focus of our future research.

Declaration of Competing Interest

The authors declare that they have no competing financial interest or personal relationships that could have appeared to influence the work reported in this article.

Acknowledgments

The authors would like to thank Prof. Zhaoheng Liu of École de Technologie Superiéure for the valuable suggestions which have improved the quality of this paper. The work was supported by NSF of China under Grant (12162006, 11802065), and the Cultivation Project of Guizhou University [2019] no. 63.

Appendix A. Detailed derivations of the related variables in Eq. (14)

$$\frac{\partial L}{\partial \dot{x}} = (2M_w + M_r + \frac{2I_w}{r^2})\frac{\cos^2(\varphi-\beta)}{\cos^2\beta}\dot{x} + M_f\dot{x},$$
$$\frac{\partial L}{\partial \dot{y}} = (2M_w + M_r + \frac{2I_w}{r^2})\frac{\cos^2(\varphi-\beta)}{\cos^2\beta}\dot{y} + M_f\dot{y},$$
$$\frac{\partial L}{\partial \dot{\theta}} = (2I_{wd} + I_{fd})\dot{\theta} + [(M_w r^2 + I_w)\frac{d^2}{2r^2} + 2I_{wd} + I_{rd}](\dot{\theta} - \dot{\varphi}),$$
$$\frac{\partial L}{\partial \dot{\varphi}} = -[(M_w r^2 + I_w)\frac{d^2}{2r^2} + 2I_{wd} + I_{rd}](\dot{\theta} - \dot{\varphi}),$$
$$\frac{\partial L}{\partial \dot{\theta}_l} = (M_w r^2 + I_w)\dot{\theta}_l,$$
$$\frac{\partial L}{\partial \dot{\theta}_r} = (M_w r^2 + I_w)\dot{\theta}_r,$$
$$\frac{\mathrm{d}}{\mathrm{d}t}\left(\frac{\partial L}{\partial \dot{x}}\right) = \frac{1}{\cos^2\beta}(2M_w + M_r + \frac{2I_w}{r^2})[\ddot{x}\cos^2(\varphi-\beta) - \dot{\varphi}\dot{x}\sin(2\varphi-2\beta) + 2\dot{x}\dot{\beta}\frac{\sin\varphi\cos(\varphi-\beta)}{\cos\beta}] + M_f\ddot{x},$$
$$\frac{\mathrm{d}}{\mathrm{d}t}\left(\frac{\partial L}{\partial \dot{y}}\right) = \frac{1}{\cos^2\beta}(2M_w + M_r + \frac{2I_w}{r^2})[\ddot{y}\cos^2(\varphi-\beta) - \dot{\varphi}\dot{y}\sin(2\varphi-2\beta) + 2\dot{y}\dot{\beta}\frac{\sin\varphi\cos(\varphi-\beta)}{\cos\beta}] + M_f\ddot{y},$$
$$\frac{\mathrm{d}}{\mathrm{d}t}\left(\frac{\partial L}{\partial \dot{\theta}}\right) = [(M_w r^2 + I_w)\frac{d^2}{2r^2} + 2I_{wd} + I_{rd}](\ddot{\theta} - \ddot{\varphi}) + (2I_{wd} + I_{fd})\ddot{\theta},$$
$$\frac{\mathrm{d}}{\mathrm{d}t}\left(\frac{\partial L}{\partial \dot{\varphi}}\right) = -[(M_w r^2 + I_w)\frac{d^2}{2r^2} + 2I_{wd} + I_{rd}](\ddot{\theta} - \ddot{\varphi}),$$
$$\frac{\mathrm{d}}{\mathrm{d}t}\left(\frac{\partial L}{\partial \dot{\theta}_l}\right) = (M_w r^2 + I_w)\ddot{\theta}_l,$$
$$\frac{\mathrm{d}}{\mathrm{d}t}\left(\frac{\partial L}{\partial \dot{\theta}_r}\right) = (M_w r^2 + I_w)\ddot{\theta}_r,$$
$$\frac{\partial L}{\partial x} = \frac{\partial L}{\partial y} = \frac{\partial L}{\partial \theta} = \frac{\partial L}{\partial \theta_r} = \frac{\partial L}{\partial \theta_l} = 0,$$
$$\frac{\partial L}{\partial \varphi} = \frac{1}{\cos^3\beta}(2M_w + M_r + \frac{2I_w}{r^2})\cos(\varphi-\beta)[\mu\sin\varphi - \sin(\varphi-\beta)\cos\beta](\dot{x}^2 + \dot{y}^2).$$

Appendix B. Coefficient matrices of Eq. (15)

$$\mathbf{A}(\mathbf{q}) = \begin{bmatrix} a_{11} & 0 & 0 & 0 & 0 & 0 \\ 0 & a_{22} & 0 & 0 & 0 & 0 \\ 0 & 0 & a_{33} & a_{34} & 0 & 0 \\ 0 & 0 & a_{43} & a_{44} & 0 & 0 \\ 0 & 0 & 0 & 0 & a_{55} & 0 \\ 0 & 0 & 0 & 0 & 0 & a_{66} \end{bmatrix}, \qquad \mathbf{U}(\mathbf{q}, \dot{\mathbf{q}}) = \begin{bmatrix} u_{11} \\ u_{21} \\ 0 \\ u_{41} \\ 0 \\ 0 \end{bmatrix},$$

with

$$a_{11} = a_{22} = (2M_w + M_r + \frac{2I_w}{r^2})\frac{\cos^2(\varphi-\beta)}{\cos^2\beta} + M_f,$$

$$a_{33} = (M_w r^2 + I_w)\frac{d^2}{2r^2} + 4I_{wd} + I_{fd} + I_{rd},$$

$$a_{34} = a_{43} = -(M_w r^2 + I_w)\frac{d^2}{2r^2} - 2I_{wd} - I_{rd},$$

$$a_{44} = (M_w r^2 + I_w)\frac{d^2}{2r^2} + 2I_{wd} + I_{rd},$$

$$a_{55} = a_{66} = M_w r^2 + I_w,$$

$$u_{11} = \frac{1}{\cos^2\beta}(2M_w + M_r + \frac{2I_w}{r^2})(\omega v\cos\theta - \frac{v^2\sin\varphi\cos\theta}{a\cos\beta})[\frac{2\mu}{1-\mu}\tan\beta\cos^2(\varphi-\beta) - \sin(2\varphi-2\beta)],$$

$$u_{21} = \frac{1}{\cos^2\beta}(2M_w + M_r + \frac{2I_w}{r^2})(\omega v\sin\theta - \frac{v^2\sin\varphi\sin\theta}{a\cos\beta})[\frac{2\mu}{1-\mu}\tan\beta\cos^2(\varphi-\beta) - \sin(2\varphi-2\beta)],$$

$$u_{41} = \frac{2}{\cos^3\beta}(2M_w + M_r + \frac{2I_w}{r^2})\cos(\varphi-\beta)[\mu\sin\varphi - \sin(\varphi-\beta)\cos\beta]v^2.$$

References

[1] A.R. Latif, N. Chalhoub, V. Pilipchuk, Control of the nonlinear dynamics of a truck and trailer combination, Nonlinear Dyn. 99 (2020) 2505–2526, doi:10.1007/s11071-019-05452-1.
[2] X.H. Li, G. Zhao, B.T. Li, Generating optimal path by level set approach for a mobile robot moving in static/dynamic environments, Appl. Math. Model. 85 (2020) 210–230, doi:10.1016/j.apm.2020.03.034.
[3] A. Astolfi, P. Bolzern, A. Locatelli, Path-tracking of a tractor-trailer vehicle along rectilinear and circular paths: a Lyapunov-based approach, IEEE Trans. Rob. Autom. 20 (2014) 154–160 1109/TRA.2014.820928.
[4] M. Abroshan, R. Hajiloo, E. Hashemi, A. Khajepour, Model predictive-based tractor-trailer stabilisation using differential braking with experimental verification, Veh. Sys. Dyn. 20 (2020) 1–24, doi:10.1080/00423114.2020.1744024.
[5] P. Fancher, C. Winkler, Directional performance issues in evaluation and design of articulated heavy vehicles, Veh. Sys. Dyn. 45 (2007) 607–647, doi:10.1080/00423110701422434.
[6] S. Vempaty, Y.P. He, L. Zhao, An overview of control schemes for improving the lateral stability of car-trailer combinations, Int. J. Veh. Perform. 6 (2020) 151–199, doi:10.1504/IJVP.2020.106985.
[7] A.K. Khalaji, S.A.A. Moosavian, Dynamic modeling and tracking control of a car with n trailers, Multibody Syst. Dyn. 37 (2016) 211–225, doi:10.1007/s11044-015-9472-9.
[8] X. Jin, J. Liang, S.L. Dai, D. Guo, Adaptive line-of-sight tracking control for a tractor-trailer vehicle system with multiple constraints, IEEE Trans. Intell. Transp. Syst. 1 (2021) 1–12, doi:10.1109/TITS.2021.3103102.
[9] J. David, P.V. Manivannan, Control of truck-trailer mobile robots: a survey, Intell. Serv. Robot. 7 (2014) 245–258, doi:10.1007/s11370-014-0152-z.
[10] J. Yuan, S.K. Yang, J.X. Cai, Consistent path planning for on-axle-hitching multi-steering trailer systems, IEEE Trans. Ind. Electron. 65 (2018) 9625–9634, doi:10.1109/TIE.2018.2823691.
[11] J. Yuan, Hierarchical motion planning for multisteering tractor-trailer mobile robots with on-axle hitching, IEEE ASME Trans. Mechatron. 22 (2017) 1652–1662, doi:10.1109/TMECH.2017.2695651.
[12] X.M. Xu, Y.P. Jiang, N. Chen, H.P. Lee, Dynamic behavior of a vehicle with rear axle compliance steering, J. Vibroeng. 19 (2017) 4483–4497, doi:10.21595/jve.2017.17580.
[13] A.K. Khalaji, Control of a tractor-trailer robot subjected to wheel slip, Proc. Inst. Mech. Eng. K. J. Multi-body Dyn. 233 (2019) 956–967, doi:10.1177/1464419319839848.
[14] K. Alipour, A.B. Robat, B. Tarvirdizadeh, Dynamics modeling and sliding mode control of tractor-trailer wheeled mobile robots subject to wheels slip, Mech. Mach. Theory 138 (2019) 16–37, doi:10.1016/j.mechmachtheory.2019.03.038.
[15] H.A. Khan, S.N. Yun, E.A. Jeong, J.W. Park, C.M. Yoo, S.M. Han, A review of rear axle steering system technology for commercial vehicles, J. Drive Control 17 (2020) 152–159, doi:10.7839/ksfc.2020.17.4.152.
[16] P. Ritzen, E. Roebroek, N.V.D. Wouw, Z.P. Jiang, H. Nijmeijer, Trailer steering control of a tractor-trailer robot, IEEE Trans. Control Syst. Technol. 24 (2016) 1240–1252, doi:10.1109/TCST.2015.2499699.
[17] P. Kassaeiyan, K. Alipour, B. Tarvirdizadeh, A full-state trajectory tracking controller for tractor-trailer wheeled mobile robots, Mech. Mach. Theory 150 (2020) 103872, doi:10.1016/j.mechmachtheory.2020.103872.
[18] P. Kassaeiyan, B. Tarvirdizadeh, K. Alipour, Control of tractor-trailer wheeled robots considering self-collision effect and actuator saturation limitations, Mech. Syst. Signal Process. 127 (2019) 388–411, doi:10.1016/j.ymssp.2019.03.016.
[19] E. Kayacan, E. Kayacan, H. Ramon, W. Saeys, Robust tube-based decentralized nonlinear model predictive control of an autonomous tractor-trailer system, IEEE/ASME Trans. Mechatron. 20 (2014) 447–456, doi:10.1109/TMECH.2014.2334612.
[20] Z.K. Jin, Z.Y. Liang, P.F. Guo, M.W. Zheng, Adaptive backstepping tracking control of a car with n trailers based on RBF neural network, Asian J. Control 23 (2021) 824–834, doi:10.1002/asjc.2255.
[21] Y.Q. Wang, B. Niu, H.Q. Wang, N. Alotaibi, E.A. Abozinadah, Neural network-based adaptive tracking control for switched nonlinear systems with prescribed performance: an average dwell time switching approach, Neurocomputing 435 (2021) 295–306, doi:10.1016/j.neucom.2020.10.023.
[22] N. Xu, B. Niu, H.Q. Wang, X. Huo, X.D. Zhao, Single-network ADP for solving optimal event-triggered tracking control problem of completely unknown nonlinear systems, Int. J. Intell. Syst. 36 (2021) 4795–4815, doi:10.1002/int.22491.
[23] B. Li, T. Acarman, Y.M. Zhang, L.L. Zhang, C. Yaman, Q. Kong, Tractor-trailer vehicle trajectory planning in narrow environments with a progressively constrained optimal control approach, IEEE Trans. Intell. Veh. 5 (2020) 414–425, doi:10.1109/TIV.2019.2960943.
[24] N.T. Binh, N.A. Tung, D.P. Nam, N.H. Quang, An adaptive backstepping trajectory tracking control of a tractor trailer wheeled mobile robot, Int. J. Control Autom. Syst. 17 (2019) 465–473, doi:10.1007/s12555-017-0711-0.
[25] Z.K. Jin, Z.Y. Liang, X. Wang, M.W. Zheng, Adaptive backstepping sliding mode control of tractor-trailer system with input delay based on RBF neural network, Int. J. Control Autom. Syst. 19 (2021) 76–87, doi:10.1007/s12555-019-0796-8.
[26] M. Yue, X.Q. Hou, W.B. Hou, Composite path tracking control for tractor-trailer vehicles via constrained model predictive control and direct adaptive fuzzy techniques, J. Dyn. Syst. Meas. Control 139 (2017) 111008, doi:10.1115/1.4036884.

[27] Y.S. Zhou, Z.H. Wang, K.W. Chung, Turning motion control design of a two-wheeled inverted pendulum using curvature tracking and optimal control, J. Optim. Theory Appl. 181 (2019) 634–652, doi:10.1007/s10957-019-01472-4.
[28] Y.S. Zhou, X.R. Wen, X. Qi, Precise motion control of tractor-trailer wheeled mobile structures via a newly observed key motion law, Nonlinear Dyn. 103 (2021) 833–848, doi:10.1007/s11071-020-06162-9.